Surface & Coatings Technology 307 (2016) 374–381

Contents lists available at ScienceDirect

Surface & Coatings Technology

journal homepage: www.elsevier.com/locate/surfcoat

Chromium interlayer amorphous carbon film for 304 stainless steel bipolar plate of proton exchange membrane fuel cell

Wu Mingge [a], Lu Congda [a,*], Hong Tao [a], Chen Guohai [a], Wen Donghui [a], Zhang Haifeng [b], Zhang Dong [b], Wang Aiying [b]

[a] College of Mechanical Engineering, Zhejiang University of Technology, Hangzhou 310014, China
[b] Key Laboratory of Marine Materials and Related Technologies, Zhejiang Key Laboratory of Marine Materials and Protective Technologies, Ningbo Institute of Materials Technology and Engineering, Chinese Academy of Sciences, Ningbo 315201, China

ARTICLE INFO

Article history:
Received 19 March 2016
Revised 22 July 2016
Accepted in revised form 23 July 2016
Available online 26 July 2016

Keywords:
Proton exchange membrane fuel cell
Amorphous carbon film
Cr interlayer
Interfacial contact resistance
Corrosion resistance
Polarization curve

ABSTRACT

Excellent electrical conductivity and corrosion resistance make the graphite-like carbon film an ideal surface modification for metal bipolar plates, but the pinhole inside amorphous carbon (a-C) causes pitting corrosion of the substrate. Chromium interlayer amorphous carbon (Cr/a-C) was prepared for 304SS bipolar plate. The interlock structure between the Cr interlayer and a-C film prevented corrosive liquid from reaching the substrate. The Cr/a-C film was prepared on 304SS by direct current magnetron sputtering. The hydrophobic property, interfacial contact resistance (ICR), and corrosion resistance of Cr/a-C 304SS were investigated and compared with those of bare 304SS and a-C 304SS. In addition, the performance and stability of the assembled single fuel cell were analyzed. Results show that the contact angle with water of Cr/a-C 304SS is 89.5°. The ICR of Cr/a-C 304SS under compaction force of 150 N/cm^2 is 16.65 mΩ cm^2, which is better than that of a-C 304SS. The SEM and TEM results reveal the interlock structure between the Cr interlayer and a-C film. This structure results in excellent corrosion resistance, corrosion potential of −0.32 V, and corrosion current density of 0.894 μA cm^{-2} in the simulated proton exchange membrane fuel cell (PEMFC). Single cell tests show that the peak power density of Cr/a-C 304SS PEMFC is 1.123 W cm^{-2}, with no observed degradation during 12 h lifetime tests. Thus, the Cr/a-C film is an ideal protective layer for 304SS bipolar plates of PEMFC.

© 2016 Elsevier B.V. All rights reserved.

1. Introduction

Proton exchange membrane fuel cell (PEMFC) is considered the next generation of power source, and the bipolar plate is a key component in PEMFCs. Traditional graphite bipolar plates possess high electrical conductivity and superior corrosion resistance, but they exhibit high manufacturing cost and poor mechanical properties. Stainless steel is an ideal material for the PEMFC bipolar plate because of its high electrical and thermal conductivity, good mechanical strength, and manufacturing ease. However, the passive film on its surface increases contact resistance. In addition, the corrosion of stainless steel bipolar plates under PEMFC working conditions can poison the membrane electrode by releasing corrosion byproducts such as Ni, Cr, and Fe, resulting in inferior fuel cell performance and durability. Therefore, surface modification or a coating protective layer is necessary to enhance the corrosion resistance of stainless steel [1–3].

Amorphous carbon (a-C) film generally refers to the categories of the amorphous carbon film material, among which graphite-like carbon (GLC) is considered an ideal candidate for surface modification of stainless steel bipolar plate [4–6], because of its compact structure, high electrical conductivity, superior corrosion resistance, and high mechanical strength with metallic plate. Show [7,8] and Kai [9] coated Ti and 316L SS with a-C film, respectively, and both reported significantly improved corrosion resistance and reduced contact resistance. Yi [10] fabricated 304SS bipolar plates with a-C film coated by closed field unbalanced magnetron sputter ion plating; assembled fuel cells showed that the a-C film has demonstrated excellent chemical stability and electrical performance. Feng [11] deposited an a-C film on 316L SS. Tests showed a stable a-C film that greatly reduces the corrosion rate. The interfacial contact resistance (ICR) test showed that the ICR of 316L SS deposited with a-C film is much lower than that of bare 316L SS.

However, corrosive liquid passes through the a-C film via pinholes under long working hours; therefore, the a-C film fails to meet DOE stability requirements. Li [12] mentioned that interlayer deposition such as Ti, Cr, W, and Si for a-C films offers enhanced adhesion between the substrate. Wang [13] used Cr as an interlayer and a Cr/C multilayer coating was prepared, in which the interface between Cr and carbon film showed interlock structures. The interlock structure blocked small crack growth of carbon film and significantly upgraded the mechanical properties of carbon film. In addition, doping Cr in a-C film influences the sp^3 and sp^2 carbon atom content and improves the ICR of the film [14].

* Corresponding author at: College of Mechanical Engineering, Zhejiang University of Technology, Hangzhou, Zhejiang 310014, People's Republic of China.
E-mail address: lcd@zjut.edu.cn (L. Congda).

http://dx.doi.org/10.1016/j.surfcoat.2016.07.069
0257-8972/© 2016 Elsevier B.V. All rights reserved.

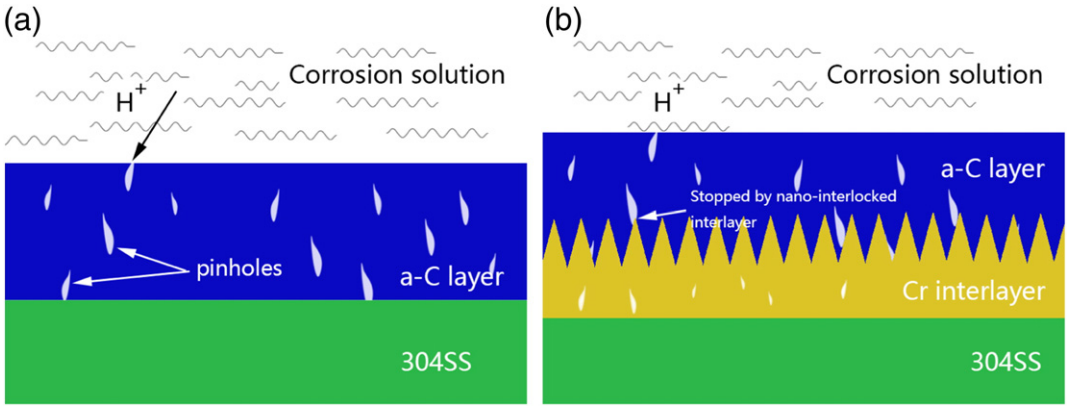

Fig. 1. (a) corrosion mechanism of a-C film and (b) corrosion resistance mechanism of interlock structure of Cr/a-C.

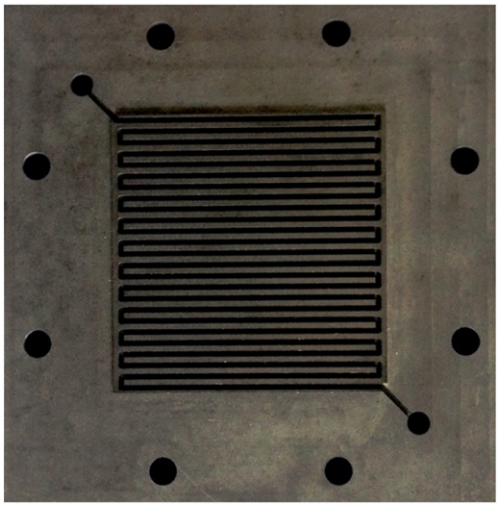

Fig. 2. Specimen of Cr/a-C 304SS bipolar plate.

In this work, a Cr/a-C film was prepared by direct current magnetron sputtering (DCMP) on 304SS substrate, and influences of the Cr interlayer were investigated from the contact angle with water, electrical conductivity, and corrosion resistance. Finally, the performance and stability of the self-assembled single fuel cell with Cr/a-C 304SS BPs were tested to verify the effects of the Cr interlayer.

2. Corrosion resistance mechanism

Under harsh acid working conditions of PEMFC, metal is in an unstable state and easily reacts with corrosive liquid, leading to corrosion of the metallic bipolar plate. At the cathode side, a passivation layer easily forms because the working potential is below the metal corrosion potential. The thin oxidation film (usually 1–3 nm) itself offers good corrosion resistance and slightly dissolves in corrosive media. Moreover, the corrosion rate is four to six orders of magnitude lower than that of metal before corrosion. However, the poor conductivity of the generated passivation layer increases the ICR between the bipolar plate and gas diffusion layer. At the anode side, metal is prone to dissolution and the dissolved metal ions are absorbed by the catalyst layer and decrease catalytic activity. This reduced activity then decreases the efficiency of the fuel cell.

The excellent chemical inertia of the a-C film makes it suitable for corrosion resistance modification of 304SS, but its internal defects such as pinholes, through which corrosive liquid reaches and comes into contact with the substrate, lead to pitting corrosion after long working hours (Fig. 1(a)). Back-diffusion Cr atoms mix with carbon atoms during magnetron sputtering. Condensation and recondensation occur on the Cr interlayer. Under appropriate sputtering current and bias voltage, the Cr layer presents typical columnar growth. A columnar

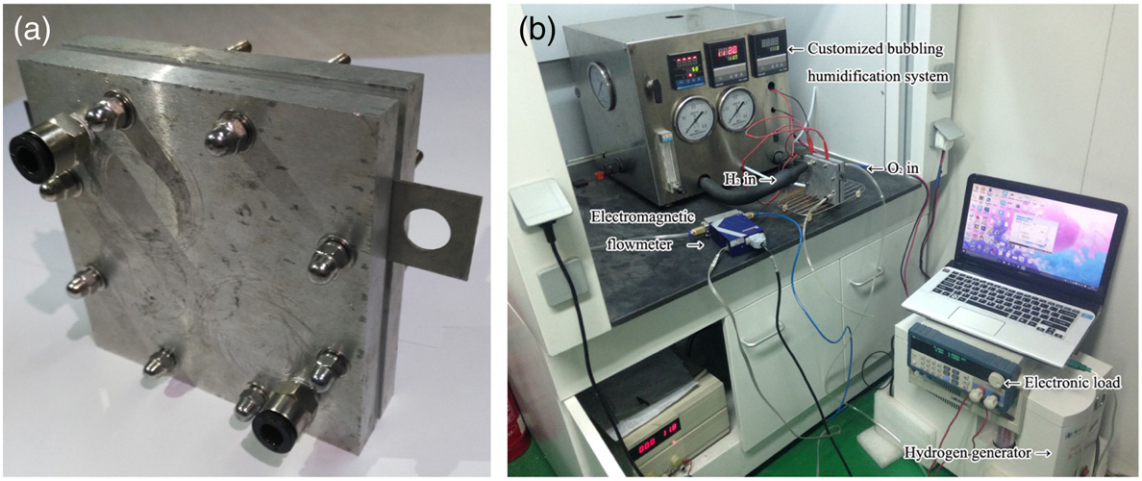

Fig. 3. Assembled PEMFC (a) and self-built PEMFC performance test system (b).

Table 1
Operating conditions for single cells tests.

Active area	25 cm^2
Operating pressure	1 atm
Operating temperature	298 K
Hydrogen flow rate	375 sccm
Air flow rate	1000 sccm
Hydrogen humidification	100%
Air humidification	50%

structure is quite compact, whereas the triangular vacancy of two cylinders is filled with a-C. Finally, the interlock structure is formed. As shown in Fig. 1(b), the internal defects of the Cr layer and a-C film are successfully staggered from the interlock structure, which effectively blocks corrosive liquid from reaching the substrate and greatly enhances corrosion resistance.

3. Experimental

3.1. Specimen preparation

An independently developed magnetic filtered cathodic arc compound sputtering deposition apparatus was selected for preparing carbon membranes. Several materials were required in substrates, such as glasses to measure resistivity of a-C film and silicon P (100) for microstructural analysis. Subsequently, the 304SS 30 mm × 30 mm substrates were polished. The substrate materials were cleaned with acetone in an ultrasonic cleaner for 15 min before coating. The experiment started after vacuum pumping to 3×10^{-5} Torr. Ar was piped at a cavity pressure of 8 mTorr. The Cr interlayer was deposited for 10 min with direct current sputtering at 3 A and bias voltage of −100 V. The bias voltage was then set to −200 V [15], and the a-C film was deposited for 60 min. For uniformity, the substrates were rotated at a constant rate during the whole preparation. Field emission scanning electron microscopy (S−4800) was employed to investigate surface and cross-sectional morphologies. Scanning probe microscopy (Dimension 3100V) was conducted to investigate the 3D topography and measure roughness. In addition, surface contact angle with water was measured by contact angle system OCA20.

3.2. Interfacial contact resistance measurements

The ICR between the specimen and conductive carbon paper (Toray TGP-H-060) was evaluated. Two pieces of carbon paper were sandwiched between two copper plates and the coated sample. A constant current of 1 A was used during the test, and the pressure was controlled by a CMT5105-type microcomputer control electronic universal testing machine. Voltage change was measured using a precision ohmmeter.

3.3. Electrochemical measurements

Electrochemical corrosion measurements were conducted by the electrochemical workstation of AUTOLAB using a three-electrode cell. A platinum electrode served as the auxiliary electrode. A saturated calomel electrode (SCE) was the reference electrode. The carbon-coated 304SS was the working electrode. The substrates were sealed with a hot glue gun that had an opening of 1 cm × 1 cm for measurement. The potentiodynamic curves were acquired at a scanning rate of 0.5 mV s^{-1} over a range of −0.7 V to 1.0 V. All electrochemical experiments were conducted in 0.5 M H_2SO_4 + 5 PPM HF solution to simulate the operational conditions of PEMFC.

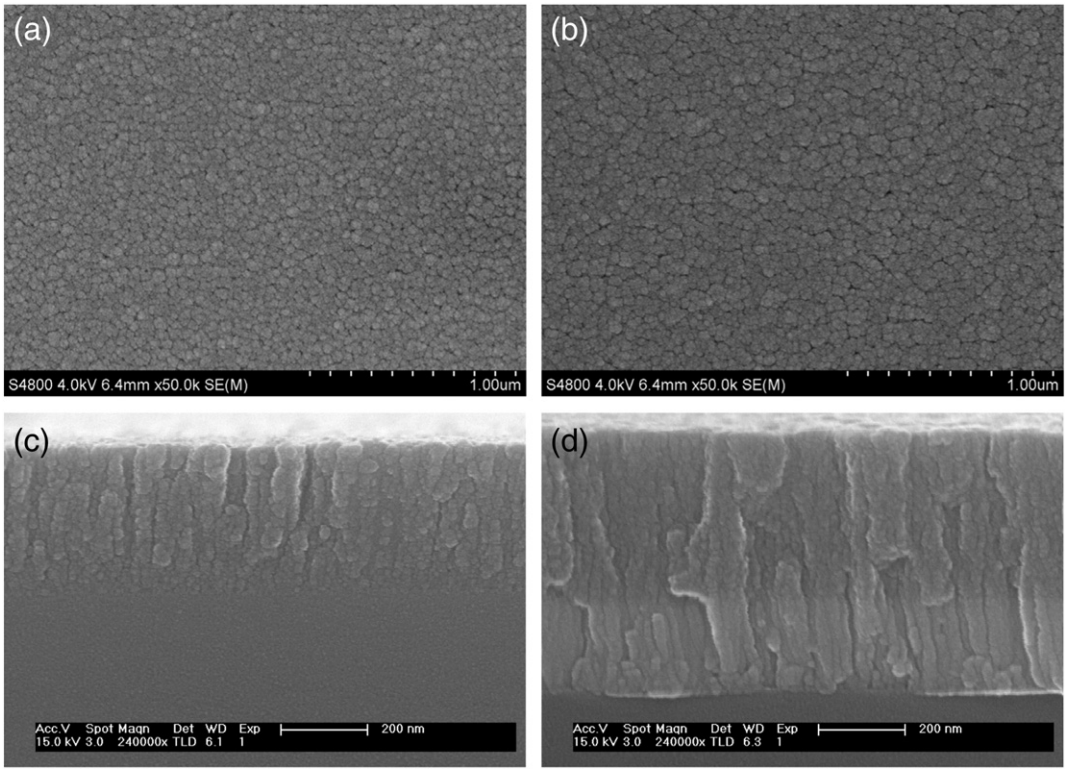

Fig. 4. SEM micrographs of surface for (a) a-C film and (b) Cr/a-C film, SEM micrographs of cross-section for (c) a-C film and (d) Cr/a-C film.

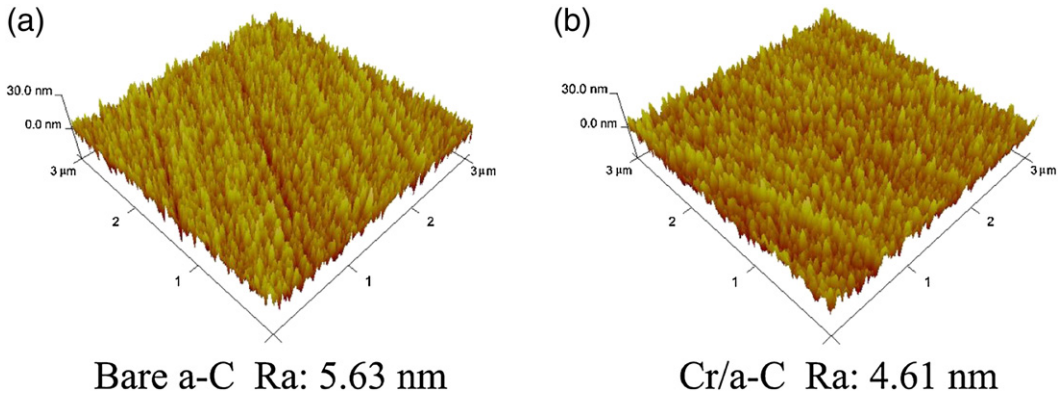

Fig. 5. SPM images and arithmetic average roughness values of random 3 μm × 3 μm areas of (a) a-C film and (b) Cr/a-C film.

3.4. Single cell tests

As shown in Fig. 2, a bipolar plate (general size of 90 mm × 90 mm; thickness of 2 mm) was designed with single serpentine flow fields. The active area is 50 mm × 50 mm. The rib width, channel width, and channel height are 1 mm. The diameter of the air inlet is 4 mm. The areas beside the active area are set to a depth of 0.55 mm for surface sealing, and eight uniform distributions via holes with diameter of 5 mm are set for positioning and assembling of the fuel cell stack.

As shown in Fig. 3, a self-assembled single cell was fabricated and tested. Commercial MEA with platinum loading of 0.5 mg cm^{-2} for anode and cathode, as well as active electrode area of 50 mm × 50 mm

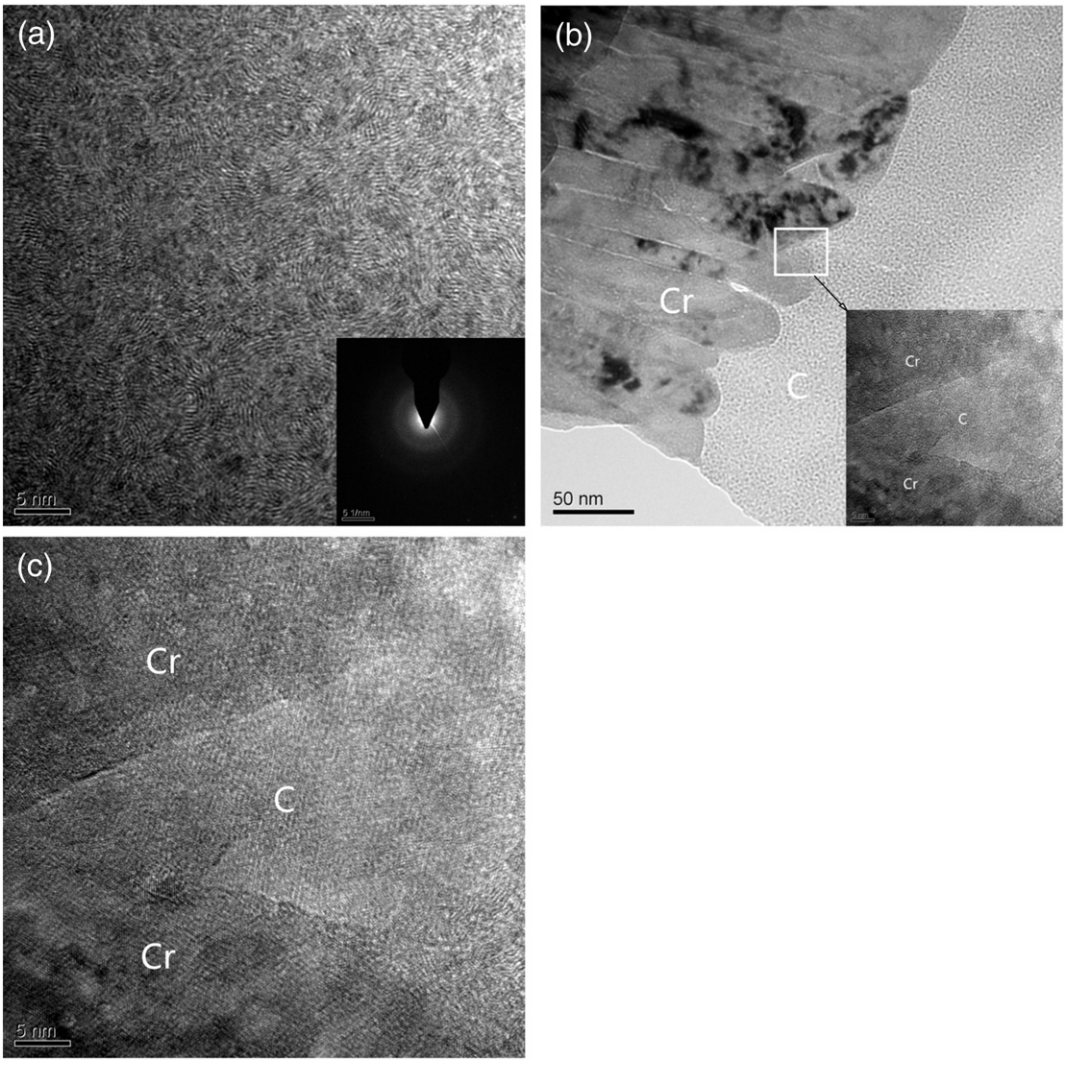

Fig. 6. High resolution TEM and electron diffraction of Cr/a-C film. (a) amorphous carbon and onion structure fullerene-like, (b) columnar crystal growth of chromium interlayer, (c) interlock structure of the interface.

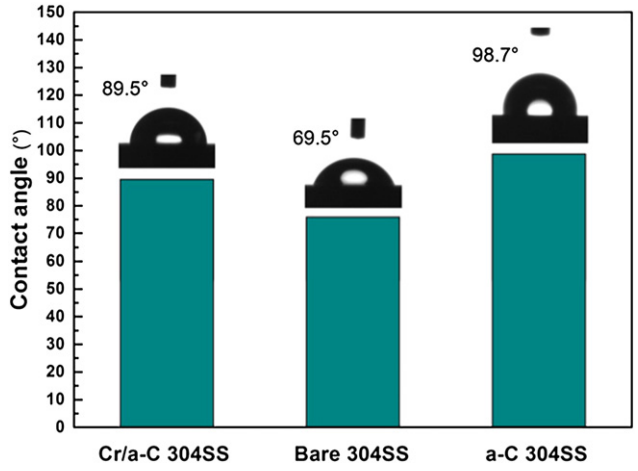

Fig. 7. Contact angles of specimens (Cr/a-C 304SS, bare 304SS and a-C 304SS) with water.

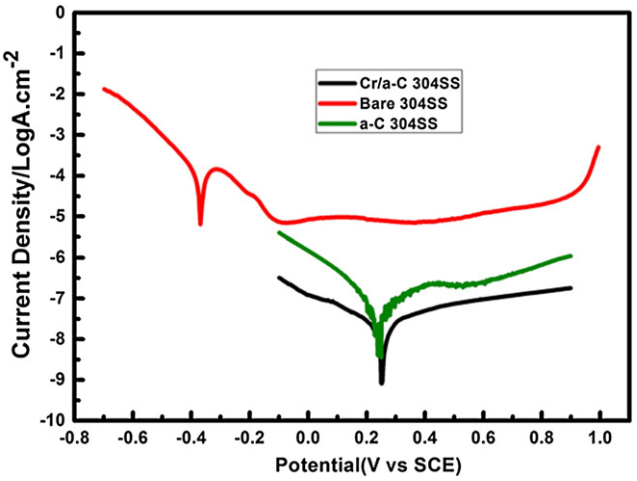

Fig. 9. Potentiodynamic polarization curves of three specimens (Cr/a-C 304SS, bare 304SS and a-C 304SS) in simulated PEMFC condition (0.5 M H_2SO_4 + 5PPM HF).

was adopted, and carbon cloths for GDL were from AvCarb. Subsequently, 10-mm-thick aluminum plates were applied as end plates. Coated bipolar plates, MEA, and silicon seals were clamped between two end plates by eight M5 screw joints. Performance was evaluated by I—V curves with a self-built system, which included a SGH-500A hydrogen generator from JieDao Tech, CS200A electromagnetic flowmeter from Sevenstar, customized bubbling humidification system, and M9711 electronic load from Maynuo. Parameters for single cell tests are shown in Table 1. Simultaneously, single cells with bare 304SS and a-C 304SS bipolar plates were also assembled and tested under the same conditions for comparison.

4. Results and discussions

4.1. Characteristics of the Cr/a-C coating

Fig. 4 presents the surface and cross-sectional morphology of pure a-C film and Cr/a-C film. The surface morphology shows that both pure a-C film and Cr/a-C film exhibit a smooth surface with no significant defects, and the surface particles of the a-C film are smaller than those of the Cr/a-C film. The thickness of the a-C film is about 400 nm, whereas that of the Cr/a-C film is about 500 nm; a high Cr sputter ionization rate is beneficial for a high deposition rate.

The scanning probe microscopy (SPM) images and arithmetic average roughness values of random (3 μm × 3 μm) areas of a-C films are presented in Fig. 5. The roughness value of the a-C film is 5.63 mm, and the roughness of the Cr/a-C film is 4.61 nm; these results correspond to the surface morphologies.

Fig. 6 shows the high-resolution TEM and electron diffraction patterns of the Cr/a-C film. Evidently, the film is an amorphous carbon with a fullerene-like structure [16]. The growth tendency of the Cr interlayer is columnar crystals, and the interface between the interlayer and carbon shows an obvious interlock structure. This structure plays a vital role in settling the pitting corrosion matter of a-C film.

4.2. Contact angle

The hydrophobic property of the bipolar plate is an important parameter for water management of PEMFC [17–19], because PEM shows better proton conductivity only in wet conditions, and reactive gases must be humidified. In addition, the electrochemical reaction of hydrogen and oxygen inside PEMFC generates extra water, which condensates to liquid water and blocks flow channels if removed in time. Hence, good hydrophobicity of the bipolar plate is beneficial to efficient water management. Fig. 7 shows the calculated values and images of the contact angle with water of the three specimens. Cr/a-C 304SS has displayed a much larger contact angle with water (about 89.5°) than bare 304SS (69.5°) but a slightly smaller angle than a-C 304SS.

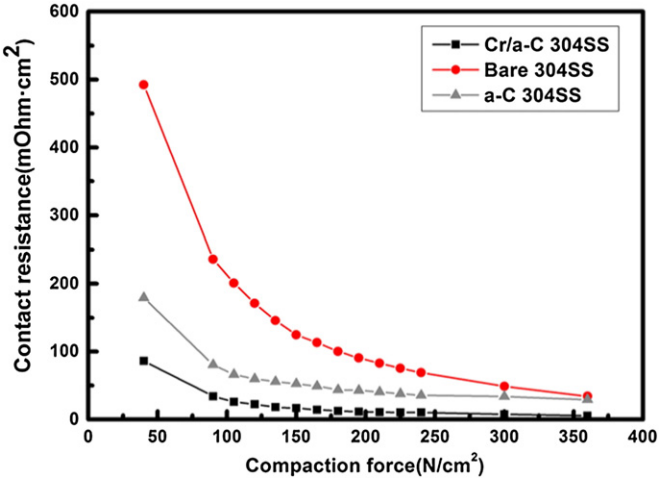

Fig. 8. ICRs of three specimens (Cr/a-C 304SS, bare 304SS and a-C 304SS) under different compaction forces (from 40 to 360 N cm^2).

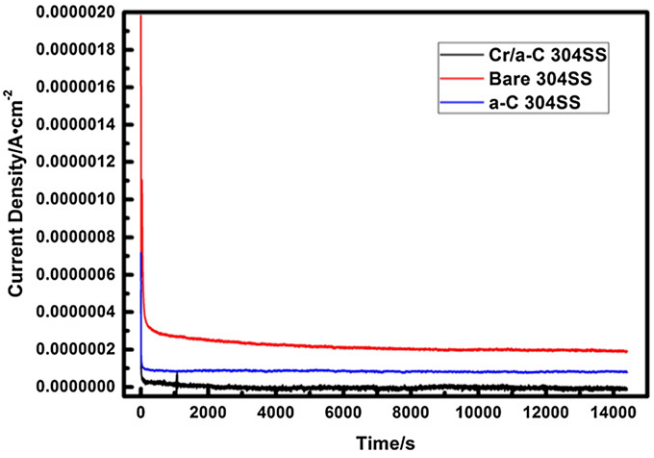

Fig. 10. Current density–time relationships of three specimens (Cr/a-C 304SS, bare 304SS and a-C 304SS) under 0.6 V_{SCE}.

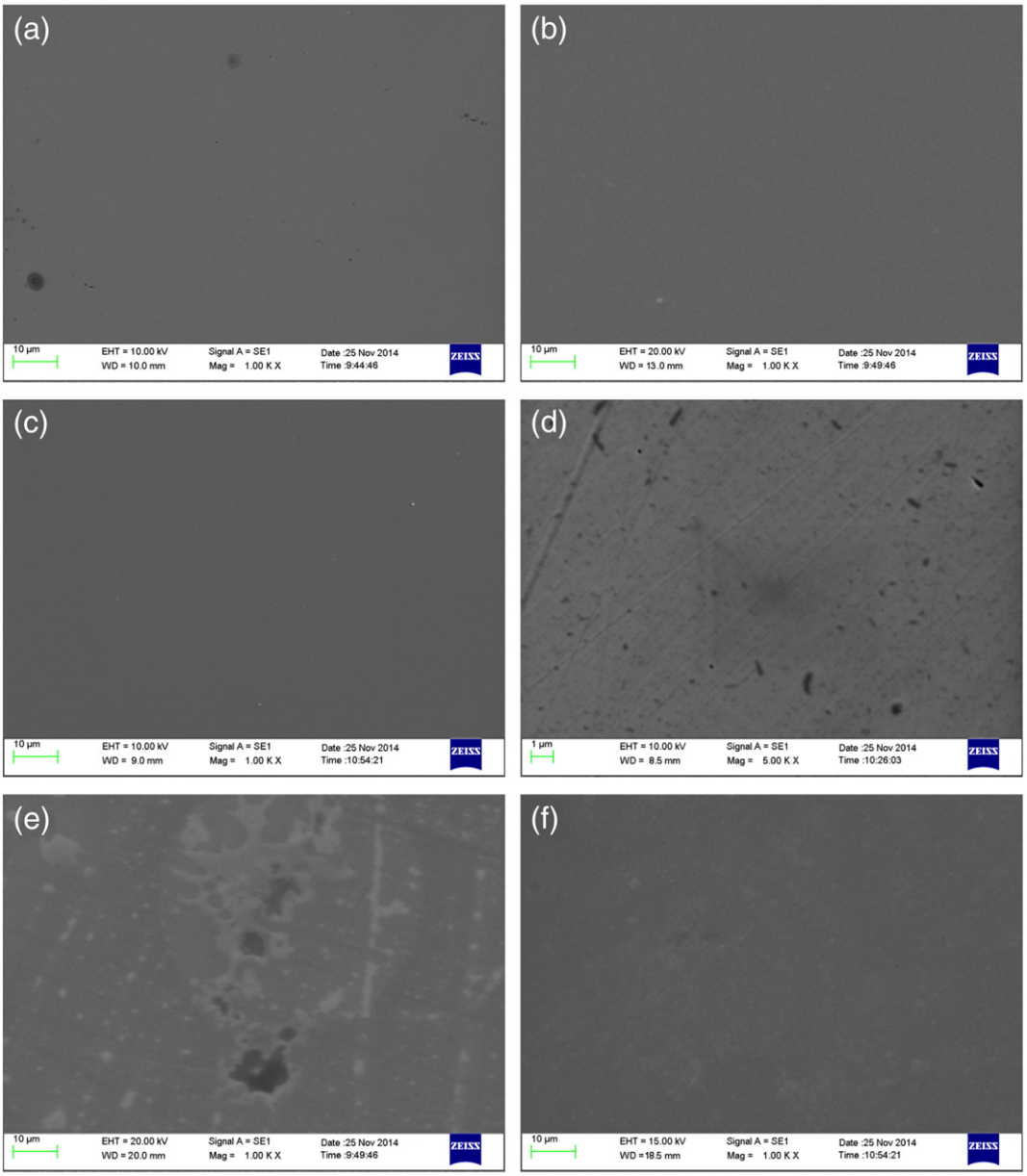

Fig. 11. SEM micrographs of surface of three specimens before potentiostatic test: (a) 304SS, (b) a-C 304SS, and (c) Cr/a-C 304SS, and after potentiostatic test: (d) 304SS, (e) a-C 304SS, and (f) Cr/a-C 304SS.

4.3. Interfacial contact resistance

High electrical conductivity is crucial to decrease ohmic loss and improve output power efficiency of PEMFC. ICR values between specimens and Toray060 carbon paper were measured under various compaction forces, as shown in Fig. 8. With increased compaction forces, the contact area of specimen and carbon paper increases, whereas contact resistance decreases. After increasing to a certain extent, the deformation of the specimen becomes infinitesimal, and the contact area is almost constant. The interface is close to near-perfect contact, and contact resistance becomes constant. The ICR of PEMFC should be less than 20 mΩ cm^2 under a compaction force of 150 N/cm^2. Bare 304SS shows a high ICR (124.4 mΩ cm^2) because of its passive film, whereas the ICR of Cr/a-C under 150 N/cm^2 is 16.65 mΩ cm^2. This value is attributed to the high percentage of sp^2 bonds in the Cr/a-C film. The ICR of Cr/a-C is much lower than that of bare 304SS but higher than that of a-C 304SS. Therefore, the Cr interlayer improves the electrical conductivity of the a-C film.

4.4. Electrochemical polarization and stability

As shown in Fig. 9, the dynamic polarization of Cr/a-C under a simulated PEMFC working environment (0.5 M H_2SO_4 + 5PPM HF) is plotted, and those of bare 304SS and a-C 304SS are provided for comparison. The corrosion resistance of the specimens is ranked in the following order: Cr/a-C 304SS > a-C 304SS > bare 304SS. The poorly compact passive film of bare 304SS is easily destroyed under cruel PEMFC working environment, which produces the corrosion potential (E_{corr}) value of −0.32 V and corrosion current density (I_{corr}) of 7.336 μA cm^{-2}. E_{corr} of a-C 304SS is 0.23 V and I_{corr} is 1.369 μA cm^{-2}, which is benefitted from the uniform and isotropic structure of amorphous property. Meanwhile, the Cr/a-C film shows good corrosion

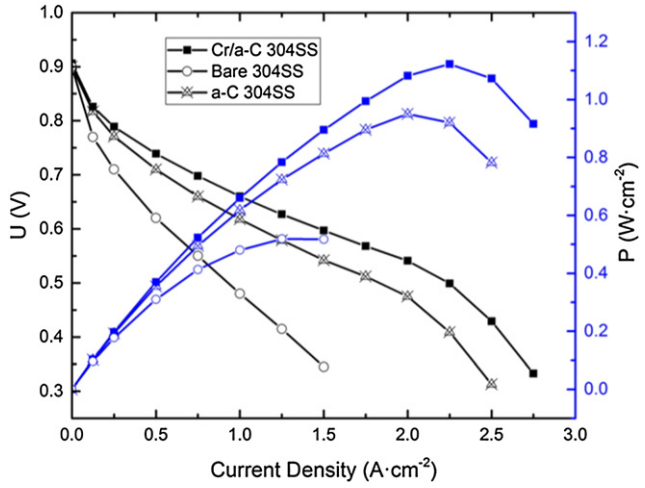

Fig. 12. Performances of assembled single fuel cells with three specimens (Cr/a-C 304SS, bare 304SS and a-C 304SS).

resistance (E_{corr} = 0.25 V, I_{corr} = 0.894 μA cm^{-2}), which is due to the interlock structure of the interface.

Potentiostatic tests were also performed to examine the stability of the specimens under a potential of 0.6 V (vs. SCE) for 4 h (Fig. 10). The current densities of the specimens initially diminish rapidly and gradually stabilize at a low level after 20–30 min. Similar to dynamic polarization, the current density of bare 304SS stabilizes at 20 μA cm^2 and a-C stabilizes at 20 μA cm^2, whereas Cr/a-C approaches 0 and then stabilizes at a negative value. The SEM micrographs presented in Fig. 11 show that large area corrosion occurs on the surface of 304SS after 4 h, which is related to the poor compactness of the passive film. The initial surface morphology of a-C 304SS is smooth but compactness is insufficient such that several tenuous holes could still be found. Corrosive liquid reaches the substrate through those small openings, causes pitting corrosion, and finally destroys the a-C film. The surface of the Cr/a-C film remains uniform and smooth without surface micropores and reveals better corrosion resistance than the a-C film.

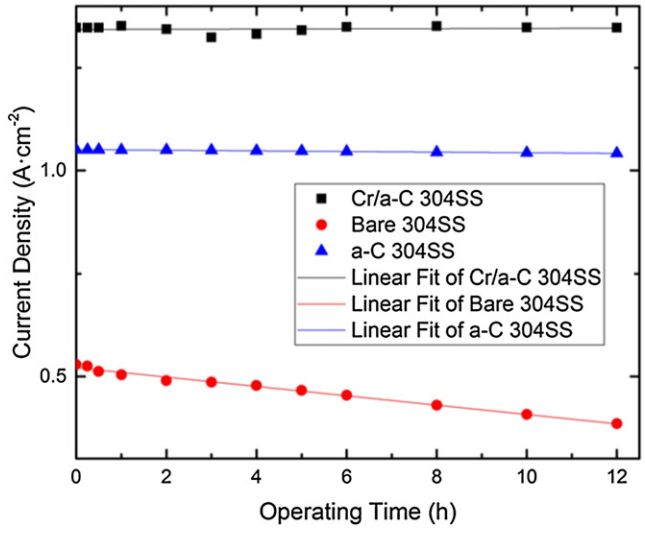

Fig. 13. Lifetime tests of assembled single fuel cells with three specimens (Cr/a-C 304SS, bare 304SS and a-C 304SS) at the operating voltage of 0.6 V during 12 h of continuous operation.

4.5. Performance and lifetime tests of single cell

Fig. 12 characterizes the polarization curves of single cells assembled with bare 304SS, a-C 304SS, and Cr/a-C 304SS bipolar plates, which all show typical polarization phenomenon. The open circuit voltage of the three fuel cells is almost the same at 0.905 V. The peak power density of the Cr/a-C 304SS fuel cell is 1.123 W cm^{-2} at a current density of 2.25 A cm^{-2}, which is better than that of a-C 304SS. The output voltage of bare 304SS and a-C 304SS attenuates faster than that of Cr/a-C 304SS, as evidenced by the ICR. This finding agrees with the results in Fig. 8. The peak current density of bare 304SS stops at 1.5 A cm^{-2}, which is related to its hydrophilicity when flooding has occurred in the flow channels.

Lifetime extension is another challenge in PEMFC. Fig. 13 compares the current density variations in the three fuel cells under an operated voltage of 0.6 V for 12 h. The current density of Cr/a-C fluctuates around 1.347 A cm^{-2}, with no tendency of degradation during the entire test time. Meanwhile, the performance degradation of the a-C 304SS fuel cell and bare 304SS is about 0.809% and 17.1%, respectively. These values are consistent with the results of Peng [10]. The lifetime tests stopped at 12 h because of the limitation of experimental conditions, but the current density of Cr/a-C 304SS stabilizes at a negative value after 30 min (Fig. 10). The performance of the Cr/a-C 304SS fuel cell may not degenerate, but further investigations are necessary.

5. Conclusions

A uniform and compact Cr/a-C film for 304SS bipolar plates of PEMFC was prepared by DCMP. The structure and performances of the film were investigated, and the following conclusions were drawn.

(1) The interface between the Cr interlayer and a-C film is an interlock structure.
(2) The contact angle with water of Cr/a-C 304SS is 89.5°, which is benefit to water management in PEMFC and anticorrosion of the bipolar plate itself.
(3) The ICR of Cr/a-C 304SS under compaction force of 150 N/cm^2 is 16.65 mΩ cm^2, which decreases by about 87% compared with the ICR of bare 304SS.
(4) The corrosion resistance of the Cr/a-C film is excellent, with corrosion potential of −0.32 V and corrosion current density of 0.894 μA cm^{-2}. Meanwhile, the current density of Cr/a-C approaches 0 and stabilize at a negative value.
(5) Single cell tests show that the peak power density of Cr/a-C 304SS PEMFC is 1.123 W cm^{-2}, which is 2.25 times that of bare 304SS and slightly better than that of a-C 304SS. No observed degradation occurred during 12 h lifetime tests, indicating the improvement in a-C 304SS.

Acknowledgement

This work is financially supported by the National Natural Science Foundation of China (51175472), Young Scholars of Zhejiang Province (R1111149).

References

[1] R. Taherian, A review of composite and metallic bipolar plates in proton exchange membrane fuel cell: materials, fabrication, and material selection[J], J. Power Sources 265 (1) (2014) 370–390.
[2] L. Peng, P. Yi, X. Lai, Design and manufacturing of stainless steel bipolar plates for proton exchange membrane fuel cells[J], Int. J. Hydrog. Energy 39 (36) (2014) 21127–21153.
[3] K. Feng, Z. Li, X. Cai, et al., Corrosion behavior and electrical conductivity of niobium implanted 316L stainless steel used as bipolar plates in polymer electrolyte membrane fuel cells[J], Surf. Coat. Technol 205 (1) (2010) 85–91.
[4] A. Liu, Q. Ren, T. Xu, et al., Morphology-controllable gold nanostructures on phosphorus doped diamond-like carbon surfaces and their electrocatalysis for glucose oxidation[J], Sensors Actuators B Chem 162 (1) (2012) 135–142.

[5] A. Liu, W. Dong, E. Liu, et al., Non-enzymatic hydrogen peroxide detection using gold nanoclusters-modified phosphorus incorporated tetrahedral amorphous carbon electrodes[J], Electrochim. Acta 55 (55) (2010) 1971–1977.
[6] A. Liu, J. Zhu, J. Han, et al., Correlation between substrate bias, growth process and structural properties of phosphorus incorporated tetrahedral amorphous carbon films[J], Appl. Surf. Sci 253 (23) (2007) 9124–9129.
[7] Y. Show, Electrically conductive amorphous carbon coating on metal bipolar plates for PEFC[J], Surf. Coat. Technol 202 (s 4–7) (2007) 1252–1255.
[8] Y. Show, M. Miki, T. Nakamura, Increased in output power from fuel cell used metal bipolar plate coated with a-C film[J], Diam. Relat. Mater 16 (s 4–7) (2007) 1159–1161.
[9] F. Kai, S. Yao, H. Sun, et al., Conductive amorphous carbon-coated 316L stainless steel as bipolar plates in polymer electrolyte membrane fuel cells[J], Int. J. Hydrog. Energy 34 (16) (2009) 6771–6777.
[10] P. Yi, L. Peng, L. Feng, et al., Performance of a proton exchange membrane fuel cell stack using conductive amorphous carbon-coated 304 stainless steel bipolar plates [J], J. Power Sources 195 (20) (2010) 7061–7066.
[11] K. Feng, X. Cai, H. Sun, et al., Carbon coated stainless steel bipolar plates in polymer electrolyte membrane fuel cells[J], Diam. Relat. Mater 19 (11) (2010) 1354–1361.
[12] Y.S. Li, Y. Tang, Q. Yang, et al., Growth and adhesion failure of diamond thin films deposited on stainless steel with ultra-thin dual metal interlayers[J], Appl. Surf. Sci 256 (24) (2010) 7653–7657.
[13] Y. Wang, J. Pu, J. Wang, et al., Interlayer design for the graphite-like carbon film with high load-bearing capacity under sliding-friction condition in water[J], Appl. Surf. Sci 311 (9) (2014) 816–824.
[14] B. Wu, G. Lin, Y. Fu, et al., Chromium-containing carbon film on stainless steel as bipolar plates for proton exchange membrane fuel cells[J], Fuel Energy Abstr 35 (35) (2010) 13255–13261.
[15] H. Zhang, D. Zhang, X. Li, et al., Electric conductivity and corrosion resistance of amorphous carbon films prepared by direct current magnetron sputtering on 304 stainless steel[J], Chin. J. Mater. Res 29 (10) (2015) 751–756.
[16] Y. Wang, J. Guo, J. Zhao, et al., Medium ion energy synthesis of hard elastic fullerene-like hydrogenated carbon film with ultra-low friction and wear in humid air[J], Mater. Lett 143 (143) (2015) 188–190.
[17] P. Yi, L. Peng, T. Zhou, et al., Development and characterization of multilayered Cr–C/a-C:Cr film on 316L stainless steel as bipolar plates for proton exchange membrane fuel cells[J], J. Power Sources 230 (10) (2013) 25–31.
[18] E.A. Cho, U.S. Jeon, H.Y. Ha, et al., Characteristics of composite bipolar plates for polymer electrolyte membrane fuel cells[J], J. Power Sources 125 (2) (2004) 178–182.
[19] Y. Zhou, B. Wang, X. Song, et al., Control over the wettability of amorphous carbon films in a large range from hydrophilicity to super-hydrophobicity[J], Appl. Surf. Sci 253 (5) (2006) 2690–2694.